

**This is an electronic reprint of the original article.  
This reprint *may differ* from the original in pagination and typographic detail.**

**Author(s):** Antenucci, Lina; Hytönen, Vesa P.; Yläne, Jari

**Title:** Phosphorylated immunoreceptor tyrosine-based activation motifs and integrin cytoplasmic domains activate spleen tyrosine kinase via distinct mechanisms

**Year:** 2018

**Version:**

**Please cite the original version:**

Antenucci, L., Hytönen, V. P., & Yläne, J. (2018). Phosphorylated immunoreceptor tyrosine-based activation motifs and integrin cytoplasmic domains activate spleen tyrosine kinase via distinct mechanisms. *Journal of Biological Chemistry*, 293(13), 4591-4602. <https://doi.org/10.1074/jbc.RA117.000660>

All material supplied via JYX is protected by copyright and other intellectual property rights, and duplication or sale of all or part of any of the repository collections is not permitted, except that material may be duplicated by you for your research use or educational purposes in electronic or print form. You must obtain permission for any other use. Electronic or print copies may not be offered, whether for sale or otherwise to anyone who is not an authorised user.

Phosphorylated immunoreceptor tyrosine-based activation motifs and integrin cytoplasmic domains activate spleen tyrosine kinase via distinct mechanisms

Lina Antenucci<sup>1</sup>, Vesa P. Hytönen<sup>2</sup> and Jari Ylännä<sup>1</sup>

<sup>1</sup>Department of Biological and Environmental Science and Nanoscience Center, University of Jyväskylä, Surfontie 9 C, P.O. BOX 35, 40014 Jyväskylä, Finland; <sup>2</sup>Faculty of Medicine and Life Sciences and BioMediTech, University of Tampere, and Finlab Laboratories, Tampere, Finland

Running title: *Role of Integrin cytoplasmic domain in Syk activation*

Author ORCID ID codes: LA: 0000-0003-1201-9342; VPH: 0000-0002-9357-1480; JY: 0000-0003-4627-021X

\*To whom correspondence should be addressed: Lina Antenucci, Department of Biological and Environmental Science and Nanoscience Center, University of Jyväskylä, Surfontie 9 C, P.O. BOX 35, 40014 Jyväskylä, Finland; [lina.antenucci@jyu.fi](mailto:lina.antenucci@jyu.fi); +358 403658477.

Keywords: Spleen Tyrosine Kinase (Syk), Integrin, enzyme kinetics, cell signaling, surface plasmon resonance (SPR)

## ABSTRACT

Spleen tyrosine kinase (Syk) is involved in cellular adhesion and also in the activation and development of hematopoietic cells. Syk activation induced by genomic rearrangement has been linked to certain T-cell lymphomas, and Syk inhibitors have been shown to prolong survival of patients with B-cell lineage malignancies. Syk is activated either by its interaction with a double-phosphorylated Immunoreceptor Tyrosine-based Activation Motif (pITAM), which induces rearrangements in the Syk structure, or by the phosphorylation of specific tyrosine residues. In addition to its immunoreceptor function, Syk is activated downstream of integrin pathways, and integrins bind to the same region in Syk as does pITAM. However, it is unknown whether integrins and pITAM use the same mechanism to activate Syk. Here, using purified Syk protein and fluorescence-based enzyme assay we investigated whether interaction of the integrin  $\beta_3$  cytoplasmic domain with the Syk regulatory domain causes changes in Syk activity similar to those induced by pITAM peptides. We observed no direct Syk activation by soluble

integrin peptide, and integrin did not compete with pITAM-induced activation even though at high concentrations, integrin cytoplasmic domain peptide competed with Syk's substrate. However, clustered integrin peptides induced Syk activation, presumably via a transphosphorylation mechanism. Moreover, the clustered integrins also activated a Syk variant in which tyrosines were replaced with phenylalanine (Y348F/Y352F), indicating that clustered integrin induced Syk activation involved other phosphorylation sites. In conclusion, integrin cytoplasmic domains do not directly induce Syk conformational changes and do not activate Syk via the same mechanism as pITAM.

Keywords: Syk – Integrin – in vitro kinetic assay

## INTRODUCTION

Spleen tyrosine kinase (Syk) is a 72 kDa cytoplasmic signaling protein discovered in bovine thymus (Yang, 1994) and forms a small family of non-receptor tyrosine kinases with

Zeta-chain associated protein kinase of 70 kDa (ZAP-70) (1). Knock out studies in mouse show that Syk is required for B cell differentiation (2). Syk<sup>-/-</sup> mice are not viable because of severe perinatal hemorrhage due to lack of separation of lymphatic and venous vasculature (3). Even though Syk<sup>-/-</sup> stem cells can give rise to all other hematopoietic cells than B cells, Syk seems to have a wide function in many hematopoietic cell types whereas the function of ZAP-70 is more restricted to T cell and NK cells (1).

Syk has an important role in cancer. In hematological malignancies Syk is mainly considered as a tumor promoter (4). A chromosomal translocation has been found in T cell leukemias leading to fusion of interleukin 2 inducible T-cell kinase (ITK) and Syk genes and to an aberrantly active Syk kinase (5). This fusion has been validated as an oncogenic driver in a mouse model (6). In many other hematological malignancies high Syk activity has been detected (4), although, to our knowledge, no human point mutations have been validated as oncogenic driver mutations. Small molecule Syk inhibitors have been designed and they were shown to prolong survival of patients (7). At the moment, Syk inhibitors have not been approved for clinical use since they are rather nonspecific and many side effects are observed (8). In solid tumors, the role of Syk is less clear than in hematological tissues. In many cases Syk expression is reduced during malignancy (e.g. (9) reviewed in (4)). Many somatic mutations have been found in Syk gene (<http://cancer.sanger.ac.uk/cosmic>) and epigenetic modification can also be responsible for alterations in the expression (10). There is some evidence that Syk can act as a tumor suppressor in breast carcinomas since it reduces cell growth when re-expressed in a breast carcinoma cell line and tested in a xenotransplantation model (11).

Syk has a C-terminal tyrosine kinase domain and an N-terminal regulatory domain formed by two Src homology 2 (SH2) domains connected by a flexible linker region called Interdomain A (IA). This tandem SH2 region (tSH2) is

connected to the kinase domain via a second linker region called Interdomain B (IB) (12). The Syk activation mechanism is mostly understood. The inactive kinase can interact through SH2 domains with phosphorylated Immunoreceptor Tyrosine-based Activation Motif (pITAM) associated with TCR, BCR and FcR receptors. Upon pITAM binding the tSH2 of Syk changes its orientation in relation to the kinase domain and allows kinase activity (12). In addition, Syk is phosphorylated by Lyn and Lck kinases and it also has an auto/trans phosphorylation activity which can lead to Syk activation independently from pITAM (13). Considering that, an “OR gate switch” model for Syk activation has been proposed (13, 14). This means that an initial activation by either pITAM binding, OR by a phosphorylation event can ultimately lead to full activity of the enzyme.

In many different biological processes ITAM-based receptor signaling is concomitant with integrin signaling. The classical example of this kind of collaboration is immunological synapse, where both  $\beta_2$  integrins and TCR are required (15, 16). In neutrophils FcR signaling is linked to both integrin  $\beta_2$  and  $\beta_3$  function (17, 18). During platelet adhesion to damaged vascular cell wall the collagen receptor GPVI/FcR $\gamma$  complex works in concert with  $\beta_1$  and  $\beta_3$  integrins (19). Clearly there are multiple crossing points between pITAM/Syk and integrin signaling pathways (reviewed in (1)). There is also a direct interaction between Syk and integrins: Syk interacts with integrin  $\beta_1$ ,  $\beta_2$ , and  $\beta_3$  cytoplasmic tails (20) and the interaction is mediated mainly by N-SH2 domain and the IA, while the C-SH2 has only a marginal role in the binding (21). On the integrin side, the last 23 amino acids of  $\beta_3$  are sufficient for binding to Syk and deletion of four C-terminal residues abolished the binding (20). There are two tyrosine residues in the Syk interacting sequence of integrin  $\beta_3$ , but the interaction does not require integrin phosphorylation. Rather, tyrosine phosphorylated integrins tails fail to interact with Syk (21). While Syk has been shown to be required for normal  $\alpha_{IIb}\beta_3$  integrin

function in platelets (22), a recent study has shown that integrin-induced Syk signaling is independent on pITAM-induced Syk activation (23). In this study, mutation of Syk N-SH2 domain that prevented phosphotyrosine binding blocked ITAM-dependent signaling in mouse platelet, but did not alter integrin-dependent Syk activation (23).

Even though integrins were found to activate Syk signaling more than two decades ago (24), it is still unclear how this activation works. More specifically, can integrins activate Syk via a similar conformational mechanism as pITAM? Are other integrin-associated kinases required for the activation? Here we used *in vitro* kinetic fluorescence-based assay to study the effect of integrin  $\beta_3$  cytoplasmic domain peptide on the activity of Syk. Our results show that soluble integrin peptides do not directly activate Syk as pITAM peptide does. On the other hand, we show that clustered integrin peptides can induce Syk activation independently of other kinases, presumably via an auto/transphosphorylation mechanism.

## RESULTS

### *Syk activity measurement using real-time fluorescence-based assay*

To study the regulation of Syk *in vitro*, we first characterized the enzymatic properties of our purified full length Syk protein. To monitor kinase activity, we used a substrate peptide with SOX fluorophore ((*S*)-2-amino-*N* <sup>$\alpha$</sup> -(9-fluorenylmethyloxycarbonyl)-3-[8-hydroxy-5-(*N,N*-dimethylsulfonamido)quinoline-2-yl] propionic acid), whose fluorescence is modulated by phosphorylation (13, 25–27) (Fig. 1). As shown before (13), purified full length Syk has low initial activity, which is enhanced in the presence of ATP after a lag period (Fig. 2A). This indicates that Syk has an intrinsic autophosphorylation or transphosphorylation activity that can initiate protein activation by phosphorylation of specific tyrosines residues along the structure (13). Because calculation of initial reaction

velocity  $v_i$  is meaningless for the inactive or partially active enzyme, we analyzed the kinetic parameters of the activated Syk that was first incubated for 30 min with ATP (Fig. 2B-D). The data were fitted to the ternary model equation since it has been previously shown that Syk kinase substrate binding fits better with ternary complex equation instead of the ping-pong model (27).  $K_m$  for SOX peptide was estimated to be  $6 \pm 1 \mu\text{M}$  and  $K_m$  for ATP was  $29 \pm 3 \mu\text{M}$ . The  $k_{cat}$ , calculated considering the initial velocity, was  $22 \pm 3 \text{ min}^{-1}$ .

### *Syk can be activated by pITAM but not by soluble integrin $\beta_3$ tails*

The interaction between the integrin cytoplasmic tail and Syk is mediated by tSH2 (21). We used surface plasmon resonance (SPR) to confirm the interaction between tSH2 and integrin  $\beta_3$  cytoplasmic tail peptide. The integrin peptide was coupled on the surface and increasing concentrations of tSH2 were injected on the sensor. The interaction had a fast, concentration dependent association phase and concentration independent dissociation phase (Fig. 3A). When the experimental data were fitted with Langmuir equation, the kinetic parameters were:  $k_{on} = 398 \pm 87 \text{ M}^{-1}\text{s}^{-1}$ ,  $k_{off} = (3.22 \pm 0.12) 10^{-3} \text{ s}^{-1}$  and  $K_D = (8.1 \pm 1.5) 10^{-6} \text{ M}$ . Since the association phase was very fast and the Langmuir model is mainly based on the equilibrium levels, we also calculated the kinetic parameters assuming single binding site and using the association and dissociation data only (Fig. 3B-E) (see *Experimental Procedure* section) (28, 29). With this method, the calculated kinetic parameters were:  $k_{on} = 604 \pm 212 \text{ M}^{-1}\text{s}^{-1}$ ,  $k_{off} = (2.68 \pm 0.20) 10^{-3} \text{ s}^{-1}$  and  $K_D = (4.44 \pm 1.55) 10^{-6} \text{ M}$ . As expected, the  $k_{off}$  values were comparable, while the  $k_{on}$  calculated with Langmuir model is half of the one calculated using first rate reaction equation. We reason that the kinetic model should in this case be more accurate. On the other hand, the calculated  $K_D$  are comparable. Thus we consider that the  $K_D$  value of  $4.44 \pm 1.55 \mu\text{M}$  is the best estimate from our data.

With  $\beta_3$  integrin/Syk interaction parameters in hand, we next compared the effect of saturating concentrations of pITAM and  $\beta_3$  integrin tail peptides on Syk activity. As expected, 10  $\mu\text{M}$  pITAM significantly reduced the lag phase on Syk activation. However, 30  $\mu\text{M}$   $\beta_3$  tail peptide failed to do so (Fig. 4A). When both peptides were present, the integrin peptide did not change the effect of pITAM. When active Syk was used in this assay in the presence of saturating concentration of SOX peptide neither pITAM nor integrin showed any effect (Fig. 4B).

To further analyze the effect of integrin  $\beta_3$  cytoplasmic tail, we investigated the possible activity modulation of active Syk. To assess the integrin effect on  $K_m$  for SOX peptide, ATP concentration was kept in saturating concentration and different concentrations of SOX peptide ranging from 1.5 to 30  $\mu\text{M}$  were tested in presence of integrin peptide (from 0 to 100  $\mu\text{M}$ ). The same experiment was done to test the effect of integrin on  $K_m$  for ATP: SOX peptide was in saturating concentration and ATP was tested from 10 to 100  $\mu\text{M}$ . The double reciprocal plots (Fig. 4C, D) are consistent with integrin being a weak competitive inhibitor for the SOX peptide and non-competitive inhibitor for ATP. However, the inhibition was only observed at high integrin concentration and the  $K_i$  values could not be accurately calculated, possibly due to poor solubility of the integrin peptide at 100  $\mu\text{M}$  concentration. This is all consistent with integrin peptide containing two tyrosine residues and being able to act as a substrate at high concentration even though both of the tyrosines are not preceded by negatively charged amino acids that are required for good Syk substrates (30). Taken together, these data show that the integrin  $\beta_3$  tail peptide does not directly activate Syk, but it may be a substrate or competitive inhibitor at high concentrations.

### *Clustered integrin $\beta_3$ tails can enhance Syk activation*

In contrast to our *in vitro* findings, assays with platelets or cultured cells have shown that integrin ligation enhances Syk activity (20, 24). This could either be mediated by other kinases activated by integrin, such as Src family kinases, or by integrin clustering. To mimic integrin clustering *in vitro*, integrin  $\beta_3$  peptide was coupled through thiol group of N-terminal cysteine on the assay plate at high concentration. The clustered integrin peptide caused significant reduction of the lag phase of Syk activity (Fig. 5A). Moreover, this effect was additive to that of soluble pITAM peptide. This is consistent with the hypothesis that recruitment of Syk to integrin clusters will enhance its transphosphorylation and thus lead to increased local activity of the enzyme. As expected, clustered integrin did not have any effect on the pre-activated Syk (Fig. 5B).

### *Syk mutant (Y348F/Y352F) can be activated by clustered integrin $\beta_3$ tails*

There are two tyrosine residues in the linker peptide of C-SH2 and the kinase domain Syk (Y348 and Y353 in human and Y342 and Y346 in mouse) that have been reported to be the main phosphorylation sites required for activation of Syk via Src-family kinases (Fig. 1). To find out if these residues are required for integrin clustering-induced activation of Syk, we studied the activation of double mutant Syk (Y348F/Y352F). Consistently with literature (12), this mutant has a low basal activity that can be enhanced by the pITAM peptide (Fig. 6A). Surprisingly, Syk (Y348F/Y352F) activation was enhanced by the clustered integrin in similar way than that of wild type Syk. This suggests that Syk clustering by integrins causes transphosphorylation of Syk activation tyrosine residues other than Y348 and Y352.

## DISCUSSION

Syk plays a crucial role in diverse types of cells and it is involved in many biological processes. In this paper we have studied the consequences of integrin cytoplasmic domain binding to the enzymatic activity of Syk. While it is well established that pITAM containing receptors induce conformational changes in the regulatory domain of Syk and thus cause direct activation of the kinase domain, it has not been studied before whether integrin cytoplasmic domain peptides binding to the same region as pITAM can do the same. We found that soluble integrin peptides were not able to induce direct activation of Syk. Instead, integrin clustering could induce autophosphorylation of Syk and thus enhance its activation. These two main findings are discussed below.

There are two pathways for the initialization of Syk activation. This property has been named the “OR gate switch” model of Syk activation (14) meaning that Syk activation can either be initialized via pITAM binding to tSH2 or via phosphorylation. The molecular details of pITAM-tSH2 interaction are known (31). Briefly, the N-SH2 interacts with the C-terminal pYxxL/I motif in ITAM receptor and the C-SH2 with the N-terminal pYxxL/I motif. The structures of two SH2s are very similar and they contain a positively charged pocket to accept the phosphotyrosine and a hydrophobic pocket to accommodate the leucine/isoleucine. It seems that for pITAM binding both SH2s are needed even if the C-SH2 seems to be more flexible and unstable compared with N-SH2 (31). As a consequence of pITAM binding, the orientation of tSH2 in relation to the kinase domain changes and this releases the hinge between two globes of the kinase leading to enhanced activity. The other arm of the “OR gate switch” model implies that at least Y348, Y352 and Y630 can be phosphorylated directly by Src family kinases such as Lyn, or auto/transphosphorylated by Syk itself. This can also lead to full activation of the enzyme independent of the interaction with pITAM (14).

Here our aim was to relate the “OR gate switch” model to integrin-mediated Syk activation. Syk interacts with integrins through tSH2 and, specifically, the N-SH2 and IA are mostly involved, while the C-SH2 has a marginal contribution (21). We confirmed the interaction between isolated tSH2 and integrin  $\beta_3$  cytoplasmic tail using SPR experiment; the measured  $K_D$  was  $4.44 \pm 1.55 \mu\text{M}$ , which indicate a medium-low affinity binding. Woodside *et al.* (21) reported a higher affinity ( $K_D$  24 nM) using different peptides and different Syk preparations. This discrepancy in the determined affinities should not affect our enzyme activation assays as we used 30  $\mu\text{M}$  concentration of integrin peptide, which should be close to saturating concentration. We found that soluble integrin cytoplasmic domain peptide did not change the lag phase of Syk activation in the way pITAM peptides did. Furthermore, integrin did not inhibit pITAM-induced activation. This is consistent with pITAM and integrins having distinct binding sites (20, 21). Our results thus indicate that integrins do not induce similar conformational changes in tSH2 as pITAM.

We also performed competition experiments using the  $\beta_3$  integrin cytoplasmic domain peptide with the active Syk kinase and its substrates ATP and the SOX peptide. In this assay integrin  $\beta_3$  peptide acted as a competitive inhibitor towards the SOX peptide and showed characteristics of uncompetitive inhibition towards the ATP. In both cases the inhibition was observed at considerably higher concentrations than the measured  $K_D$  for the integrin binding to the tSH2 of Syk. Due to technical problems related to low inhibitory activity, we were not able to calculate  $K_i$  values using these data. The simplest explanation of the observed effect is that the tyrosine containing sequences in the integrin peptide can compete with the substrate peptide. Similar behavior has been observed earlier with ITAM peptides: even though they do not contain the optimal Syk substrate recognition sequences, at high concentrations they reduce Syk activity (13). Whether this phenomenon has any

relevance to physiological Syk function, remains unclear.

To study the possible contribution of integrin binding to the other arm of the “OR gate switch” model, we mimicked integrin clustering *in vitro* by coupling the  $\beta_3$  cytoplasmic domain peptide via its N-terminus to the surface of the enzymatic assay plate. Integrin clustering is the basis of many, if not all, integrin adhesion-induced signaling events (32). Integrin clustering is partly mediated by extracellular ligands, partly by adhesion components such as talin and kindlin, and partly by actin cytoskeleton (33). Integrin clusters are dynamic structures where several components are exchanged rapidly (33, 34). We found that clustered integrin peptides significantly reduced the lag phase of Syk autoactivation. This effect was additive with the pITAM-induced activation. We take this as an evidence that integrin clustering rapidly induces Syk transphosphorylation by bringing several kinase molecules in the close proximity, leading to increased local concentration (Fig. 7). We also found that the Syk (Y438F/Y352F) mutant could be activated by clustered integrins. This shows that in addition to the main regulatory Tyrosines Y348 and Y352, there are other residues that can be transphosphorylated by the Syk itself and that activate the kinase. While it has been shown that activation loop tyrosines Y525 and Y526 have little effect on Syk activity, it is well established that the C-terminal tyrosines Y630 and Y631 can stabilize the closed, inactive conformation of the enzyme (12, 35), and thus phosphorylation of these could induce the activity of even the Y438F/Y352F mutant. In mouse, Syk residues corresponding to Y630 and Y631 have been found to be autophosphorylated or transphosphorylated (36).

In conclusion, enzyme kinetic studies presented here imply that integrin cytoplasmic domain peptides do not induce direct conformational changes in Syk and do not lead to its activation with a similar mechanism as pITAM. Instead, we propose that integrin clusters may increase

the local concentration of Syk and enhance its activity via increased transphosphorylation.

## EXPERIMENTAL PROCEDURE

### *Syk full length expression and purification*

Spleen tyrosine kinase (EC 2.7.10.2) sequence cDNA (UniProt ID: P43405) was obtained from Origene Technologies Inc, (Rockville, MD) and fragment containing amino acids 1-635 was expressed with cleavable N-terminal 6xHistidine tag (MSGSHHHHHHGSSGENLYFQ/SL where / denotes TEV cleavage site) with pFastBac NT-TOPO (Bac-To-Bac expression system, Invitrogen, Thermo Fisher Scientific Inc.). The sequence of the expression construct was verified by Sanger sequencing. *Spodoptera frugiperda* (Sf9) insect cells were transfected using Cellfectin II reagent (Thermo Fisher Scientific Inc.) using manufacturer’s protocol. Recombinant protein was expressed as described previously (37). Cells were harvested 72 h after infection (multiplicity of infection, MOI=1) by centrifugation at 500 x g and resuspended in cold lysis buffer (50 mM Na-Phosphate, 500 mM NaCl, 5 mM MgCl<sub>2</sub>, 0.1% NP40, 1 mM dithiothreitol (DTT), pH 8); Pierce™ Universal Nuclease for Cell lysis (ThermoFisher) 25 U/ml and protease inhibitors tablet (cOmplete™ Protease Inhibitor cocktail, Sigma) were added separately to resuspended cells. 5 ml of lysis buffer were used for gram of wet mass. Cells were sonicated (10 times, 1 sec pulse) in ice, and then cells suspension was clarified by centrifugation at 100,000 x g for 1 h, 4 °C. Supernatant was loaded on pre equilibrated (50 mM Na-Phosphate, 500 mM NaCl, 10 mM Imidazole, pH 8) His Trap FF, 1 ml prepacked column (GE Healthcare Inc) with peristaltic pump at 0.5 ml/min flow rate, 4 °C. Column was washed with binding buffer and protein was eluted by step-wise Imidazole gradient (10, 20, 50, 100, 250 and 500 mM Imidazole in 50 mM Na-Phosphate, 500 mM NaCl, pH 8). Fractions containing Syk were pooled and concentrated

using Amicon<sup>®</sup> Ultra 15 ml Centrifugal Filter, 30 kDa cut off (Merck KGa). Protein was then loaded on HiLoad 10/30 Superdex 200 column (GE Healthcare Inc) equilibrated with 10 mM Hepes, 150 mM NaCl, 10% Glycerol, 10 mM Methionine, 1 mM DTT, pH 7.5. Protein was concentrated to final concentration of 2 mg/ml; aliquots were frozen in liquid nitrogen and stored in -80 °C.

Syk mutant (Y348F/Y352F) was obtained with QuikChange Multi Site-Directed Mutagenesis Kit (Agilent Technologies Inc) using wild type Syk as template. Sf9 insect cells were harvested after 48 h infection (MOI=3) and lysed as described for Syk wild type. Protein was purified as the wild type except that the affinity purified protein was incubated with Tobacco Etch virus protease (TEV) over-night at 4 °C to remove the 6xHistidine tag. Protein was then concentrated and loaded on gel filtration as described for Syk wild type. Final protein preparation was concentrated to 1 mg/ml. The final protein sequence contains Leu-Ser sequence left from TEV recognition site.

#### *Tandem SH2 domains expression and purification*

Tandem SH2 (amino acids 9-264) was cloned in plasmid pGTvL1-SGC plasmid (Structural Genomics Consortium, University of Oxford) using ligation-independent method (38). The final construct was sequence verified. The final protein sequence contains a Ser-Met sequence left from the vector. tSH2 were expressed using *Escherichia coli* BL21 gold cells (Agilent Technologies Inc) at 30 °C for 4 h with 0.4 mM isopropyl  $\beta$ -D-1-thiogalactopyranoside (IPTG). The bacterial pellet was lysed using French press. The protein was captured with glutathione-agarose column (Protino glutathione-agarose 4B, Macherey- Nagel GmbH) equilibrated with 20 mM Tris, 100 mM NaCl, 1 mM DTT, pH 8 and then eluted using same buffer containing 50 mM glutathione. GST-tSH2 complex was cut using TEV protease (Invitrogen), and further purified by size exclusion chromatography with a HiLoad

26/60 Superdex 75 column (GE Healthcare) in 20 mM Tris, 100 mM NaCl, 1 mM DTT, pH 8. The final protein preparation was concentrated using Amicon<sup>®</sup> Ultra Centrifugal Filter, 30 kDa cut off to 30 mg/ml. Aliquots were frozen in liquid nitrogen and stored in -80 °C.

#### *MS data acquisition and processing*

Purified proteins were analyzed by mass spectrometry using a Q-ToF type instrument (Waters Synapt G1) connected to an Acquity (Waters) UPLC chromatography system equipped with a C4 reversed phase column (Waters BEH300 C4 1.7  $\mu$ m, 2.1  $\times$  100 mm). Protein samples were diluted 10-fold with 0.1% trifluoroacetic acid (TFA) and 3  $\mu$ l aliquots were injected. The eluents were 0.1% formic acid in water (A) and 0.1% formic acid in acetonitrile (B). The gradient was from 3 to 60% B over 8 min. The mass spectrometer was tuned for detection of proteins to take 1 s lock mass (Leu enkephalin) corrected scans in the mass range from 500 to 2000 m/z. Combined mass spectra for the chromatographic peaks were deconvoluted using the MaxEnt 1 algorithm as part of Masslynx (Waters). For tSH2 the measured molecular weight was 29160 Da (expected 29163 Da), for Syk WT was 74443 (expected: 74525 Da) and for Syk FF was 72230 Da (expected 72234 Da).

#### *Surface Plasmon Resonance*

The SPR experiment was done using Biacore X instrument (GE Healthcare Inc). Integrin  $\beta_3$  cytoplasmic tail peptide (UniProt ID: [P05106](#) CKFEEERARAKWDTANNPLYKEATSTFT NITYRGT, ProteoGenix, Schiltigheim, France) was coupled onto CM5 (GE) chips using thiol coupling. The immobilization step was done at 5  $\mu$ l/min flow rate with single flow cell. The carboxymethyl-dextran surface was activated using 1:1 ratio of 0.4 M 1-Ethyl-3-(3-dimethylaminopropyl) carbodiimide EDC and 0.1 M *N*-Hydroxysuccinimide NHS for 10 minutes. Then, 0.1 M Ethylenediamine, 0.1 M sodium borate pH 8.5 for 7 minutes and 1 M Ethanolamine pH 7 for 10 minutes were



injected. To introduce thiol-reacting groups the surface was coupled with 50 mM Sulfo-GMBS (N-[ $\gamma$ -maleimidobutyryloxy]succinimide) in 0.1 M sodium borate pH 8.5 for 4 minutes. The peptide was diluted using 10 mM Hepes, pH 7 at concentration of 50  $\mu$ g/ml and injected for 10 minutes to maximize the reactivity with sulfo-GMBS. Finally, the surface was blocked with 50 mM cysteine, 1 M NaCl, 0.1 M sodium acetate, pH 4 for 4 minutes. The experiment with tSH2 was carried out with 10 mM Hepes, 150 mM NaCl, pH 7.5 as running buffer and flow rate of 10  $\mu$ l/min using two flow-cells. 2-fold dilutions of tSH2 were prepared in the running buffer starting from 1.6 to 100  $\mu$ M. Each sample was injected for 6 minutes with a delayed wash of 150 seconds. No surface regeneration was done between injections. Each measurement was done at least three times and using different chips. The final Resonance Units (RU) were obtained by subtracting the binding response obtained with the nonfunctionalized sensor from that obtained from the Integrin  $\beta_3$  cytoplasmic tail peptide-coupled cell. The original response curve were fit using Langmuir model using Biacore evaluation software 3.1 provided by the manufacturer. The data were then analysed following the method previously described (28, 29). Briefly, to calculate the association rate  $k_{on}$  of complex Integrin peptide/tSH2 the data from 10 to 30 seconds after injection were used. First the plot of  $dRU/dt$  (variation of RU in time) versus RU was done, and then the slopes obtained from linear regressions were replotted against the tSH2 concentrations used. The  $k_{on}$  is calculated based on this equation:

$$\text{Slope} \left( \frac{dRU}{dt} \text{ vs } RU \right) = k_{on} \times C + k_{off} \quad (1)$$

Where  $k_{on}$  is the association constant, C is the protein concentration injected, and  $k_{off}$  is an estimation of the dissociation rate of the complex. Since the dissociation rate is not dependent on protein concentration it can be obtained using first-rate reaction equation:

$$\ln \left( \frac{R_1}{R_t} \right) = k_{off} \times t \quad (2)$$

Where  $R_1$  is the RU at the end of sample injection,  $R_t$  is the RU at the time  $t$  and  $k_{off}$  is the dissociation constant. The  $K_d$  is equal to  $k_{off}/k_{on}$ . Data analysis was performed using linear regression.

#### *Fluorescence-based kinetic assay*

Kinetic measurements of Syk were done using SOX fluorescent peptide (25, 26). The SOX peptide used was Ac-EEEEYIQ-[DPro-Sox-G]-NH<sub>2</sub> (Sigma-Aldrich) (27). The assay was performed in SOX assay buffer (20 mM Hepes, 0.1 mM Ethylene glycol-bis( $\beta$ -aminoethyl ether)-N,N,N',N'-tetraacetic acid (EGTA), 1 mM MgCl<sub>2</sub>, 10  $\mu$ M Na-Ortho-Vanadate, 5 mg/ml BSA, 1 mM Dithiothreitol, pH 7.15) in a final volume of 50  $\mu$ l. The fluorescence was detected with Victor<sup>TM</sup> X4 2030 Multilabel Reader (Perkin Elmer) using 355 nm as excitation wavelength and 460 nm as emission wavelength in 96-well black plates at 30 °C. Data were collected every 30 seconds for at least 50 minutes. Each experiment was repeated six times and each measurement within an experiment was done in quadruplicate. Standard deviation was calculated using the data from six different experiments. Data were analysed using Repeated Measurements one way ANOVA (RM-ANOVA) followed by Tukey's multiple comparison test using GraphPad Prism 7. To conduct the ANOVA analysis data were first normalized to the highest measured product concentration in presence of pITAM and Integrin and then arcsine transformed.

#### *Syk auto/trans phosphorylation*

Syk autophosphorylation was performed as previously described with some modifications (13). Syk wild type 2.7  $\mu$ M was incubated for 30 minutes at room temperature in presence 100  $\mu$ M of ATP, in a buffer containing 15 mM Hepes, 20 mM NaCl, 10 mM MgCl<sub>2</sub>, 1 mM EGTA, 10  $\mu$ M Na Ortho-Vanadate, 10%

Glycerol, pH 7.4 in a final volume of 2 ml. After incubation, the excess of ATP was washed away using PD10 Desalting Column (GE Healthcare Inc) using the same buffer and the protein was concentrated to 0.2 mg/ml with Amicon<sup>®</sup> Ultra Centrifugal Filter, 30 kDa cut off.

#### *Kinetic measurements of Syk activity and two-substrate analysis*

Syk kinetic measurements were performed following the increase of the peptide fluorescence in the time as above described in presence of 10  $\mu$ M SOX peptide and 25  $\mu$ M ATP. Basal Syk and active Syk were used at concentration of 17 nM except for two substrate analysis where active kinase was used at 4 nM; the reaction was started by adding ATP as last ingredient. Each measurement was done at least in triplicate; a blank without Syk was recorded also and it was subtracted from the fluorescence measured in presence of the kinase. The two-substrate analysis was used to determine the  $K_m$  for ATP and SOX peptide. Hence, in the case of  $K_m$  for ATP, the ATP concentration was varied from 5 to 75  $\mu$ M in presence of a constant concentration of SOX peptide (from 1.5 to 30  $\mu$ M). Likewise,  $K_m$  for SOX was determined changing SOX peptide concentration from 1.5 to 10  $\mu$ M in presence of a constant concentration of ATP (from 5 to 75  $\mu$ M). The data were analyzed assuming that the ternary complex model describes the Syk kinetic mechanism (27):

$$v = \frac{V_{max}[ATP][SOX]}{[ATP][SOX] + [ATP]K_m^{SOX} + [SOX]K_m^{ATP} + K_m^{ATP}K_a^{SOX}} \quad (3)$$

Where  $K_m^{SOX}$  and  $K_m^{ATP}$  are Michaelis-Menten constants of SOX and ATP, respectively, and  $K_a^{SOX}$  is the association constant of SOX for Syk.  $K_m$  for ATP and SOX peptide were calculated using the following equations derived from equation (3) assuming that one of the two substrates is kept in a constant concentration:

$$\frac{1}{V_{maxapp}} = \frac{K_m^{SOX}}{V_{max}} \frac{1}{[SOX]} + \frac{1}{V_{max}} \quad (4)$$

$$\frac{1}{V_{maxapp}} = \frac{K_m^{ATP}}{V_{max}} \frac{1}{[ATP]} + \frac{1}{V_{max}} \quad (5)$$

where  $V_{maxapp}$  corresponds to the apparent rate of the reaction in presence of a constant concentration of the other substrate.

#### *Effect of pITAM and Integrin $\beta_3$ cytoplasmic tail on kinase activation and on Syk activity*

Basal and active Syk were tested in presence of pITAM peptide from CD3 $\epsilon$  chain (UniProt ID: P07766, NPDpYEPIRKGQRDLpYSGLNQR, ProteoGenix) and in presence of integrin  $\beta_3$  cytoplasmic tail peptide. Both peptides were dissolved in water and added to the reaction mix. The assay was performed as described above. pITAM peptide and integrin  $\beta_3$  cytoplasmic tail peptide were used at concentrations of 10  $\mu$ M and 30  $\mu$ M, respectively; both basal and active Syk were 17 nM. Differently, the inhibition analysis was done using active Syk at concentration of 4 nM. Hence, to test the effect of integrin  $\beta_3$  cytoplasmic tail peptide on Syk affinity for SOX peptide, the ATP concentration was kept constant to 250  $\mu$ M (saturating concentration), SOX was varied from 1 and 30  $\mu$ M and integrin peptide from 0 to 100  $\mu$ M. Similarly, to assess the integrin peptide effect on Syk affinity for ATP the SOX peptide concentration was kept constant equal to 30  $\mu$ M (saturating concentration) and ATP concentration ranged from 10 and 100  $\mu$ M.

#### *Effect clustered integrin $\beta_3$ cytoplasmic tails on kinase activation*

Integrin  $\beta_3$  cytoplasmic tail peptide was coupled on the surface of the assay plate through thiol coupling. Pierce<sup>™</sup> Maleimide Activated Plates (Thermo Scientific) were used for coupling reaction following the methods suggested from the manufacturer with minor changes. Plate was first washed with washing buffer (0.1 M Na Phosphate, 0.15 M NaCl, pH 7.2); peptide was diluted with coupling buffer (0.1 M Na Phosphate, 0.15 M NaCl, 10 mM EGTA, pH 7.2) at concentration of 5  $\mu$ M and incubated for

two hours on plate shaker. Then, the not-reacted groups were blocked with 10 µg/ml Cysteine-HCl in coupling buffer. Finally, the plate was washed and dried by centrifugation upside-down at 1000 x g. The SOX peptide based assay was performed as described before except for the absence of DTT in the assay buffer.

#### *Effect of pITAM and integrin β<sub>3</sub> cytoplasmic tail on Syk mutant (Y348F Y352F)*

To assess the effect of pITAM and integrin β<sub>3</sub> cytoplasmic tail peptide on Syk mutant activity it was used the same procedure described for Syk wild type. Syk mutant was used at concentration of 17 nM and pITAM and integrin peptide at 10 and 30 µM, respectively. The same procedure was also used in presence of integrin β<sub>3</sub> cytoplasmic tail peptide coupled on the surface.

#### ACKNOWLEDGMENTS

We thank Dr Ulrich Bergmann, (Faculty of Biochemistry and Molecular Medicine, and Biocenter Oulu, University of Oulu, Finland) for the Mass Spetctrometry analysis. Arja

Mansikkaviita, Petri Papponen (U. Jyväskylä) and Latifeh Azizi (U. Tampere) are acknowledged for technical support. Dr Ville Paavilainen (University of Helsinki) is acknowledged for advice with Baculovirus expression system. Dr. Tatu Haataja (University of Jyväskylä), and Professor Susanna Fagerholm (University of Helsinki) are acknowledged for helpful comments. The research has been funded by Academy of Finland (grant 278668 to JY and grant 290506 to VPH) and by a research sabbatical grant from Jenny and Antti Wihuri foundation to JY.

#### CONFLICT OF INTEREST

The authors have no conflict of interest

#### AUTHOR CONTRIBUTIONS

LA planned and performed all experiments and wrote the manuscript together with other authors. JY supervised the project, planned the experiments with the other authors and wrote the manuscript with other authors. VPH planned the SPR experiments with other authors, helped with the SPR, and wrote the paper with other authors.

#### REFERENCES

1. Mócsai, A., Ruland, J., and Tybulewicz, V. L. J. (2010) The SYK tyrosine kinase: a crucial player in diverse biological functions. *Nat. Rev. Immunol.* **10**, 387–402
2. Cheng, A. M., Rowley, B., Pao, W., Hayday, A., Bolen, J. B., and Pawson, T. (1995) Syk tyrosine kinase required for mouse viability and B-cell development. *Nature.* **378**, 303–306
3. Abtahian, F., Guerriero, A., Sebzda, E., Lu, M.-M., Zhou, R., Mocsai, A., Myers, E. E., Huang, B., Jackson, D. G., Ferrari, V. A., Tybulewicz, V., Lowell, C. A., Lepore, J. J., Koretzky, G. A., and Kahn, M. L. (2003) Regulation of blood and lymphatic vascular separation by signaling proteins SLP-76 and Syk. *Science.* **299**, 247–251
4. Krisenko, M. O., and Geahlen, R. L. (2015) Calling in SYK: SYK's dual role as a tumor promoter and tumor suppressor in cancer. *Biochim. Biophys. Acta BBA - Mol. Cell Res.* **1853**, 254–263
5. Streubel, B., Vinatzer, U., Willheim, M., Raderer, M., and Chott, A. (2006) Novel t(5;9)(q33;q22) fuses ITK to SYK in unspecified peripheral T-cell lymphoma. *Leukemia.* **20**, 313–318
6. Dierks, C., Adrian, F., Fisch, P., Ma, H., Maurer, H., Herchenbach, D., Forster, C. U., Sprissler, C., Liu, G., Rottmann, S., Guo, G.-R., Katja, Z., Veelken, H., and Warmuth, M. (2010) The ITK-SYK Fusion oncogene induces a T-Cell lymphoproliferative disease in mice mimicking human disease. *Cancer Res.* **70**, 6193–6204

7. Friedberg, J. W., Sharman, J., Sweetenham, J., Johnston, P. B., Vose, J. M., LaCasce, A., Schaefer-Cuttillo, J., Vos, S. D., Sinha, R., Leonard, J. P., Cripe, L. D., Gregory, S. A., Sterba, M. P., Lowe, A. M., Levy, R., and Shipp, M. A. (2010) Inhibition of Syk with fostamatinib disodium has significant clinical activity in non-Hodgkin lymphoma and chronic lymphocytic leukemia. *Blood*. **115**, 2578–2585
8. Liu, D., and Mamorska-Dyga, A. (2017) Syk inhibitors in clinical development for hematological malignancies. *J. Hematol. Oncol.* **10**, 145
9. Moroni, M., Soldatenkov, V., Zhang, L., Zhang, Y., Stoica, G., Gehan, E., Rashidi, B., Singh, B., Ozdemirli, M., and Mueller, S. C. (2004) Progressive loss of Syk and abnormal proliferation in breast cancer cells. *Cancer Res.* **64**, 7346–7354
10. Yuan, Y., Mendez, R., Sahin, A., and Dai, J. L. (2001) Hypermethylation leads to silencing of the SYK gene in human breast cancer. *Cancer Res.* **61**, 5558–5561
11. Coopman, P. J. P., Do, M. T. H., Barth, M., Bowden, E. T., Hayes, A. J., Basyuk, E., Blancato, J. K., Vezza, P. R., McLeskey, S. W., Mangeat, P. H., and Mueller, S. C. (2000) The Syk tyrosine kinase suppresses malignant growth of human breast cancer cells. *Nature*. **406**, 742–747
12. Grädler, U., Schwarz, D., Dresing, V., Musil, D., Bomke, J., Frech, M., Greiner, H., Jäkel, S., Rysiok, T., Müller-Pompalla, D., and Wegener, A. (2013) Structural and biophysical characterization of the Syk activation switch. *J. Mol. Biol.* **425**, 309–333
13. Tsang, E., Giannetti, A. M., Shaw, D., Dinh, M., Tse, J. K. Y., Gandhi, S., Ho, H., Wang, S., Papp, E., and Bradshaw, J. M. (2008) Molecular mechanism of the Syk activation switch. *J. Biol. Chem.* **283**, 32650–32659
14. Bradshaw, J. M. (2010) The Src, Syk, and Tec family kinases: Distinct types of molecular switches. *Cell. Signal.* **22**, 1175–1184
15. Monks, C. R. F., Freiberg, B. A., Kupfer, H., Sciaky, N., and Kupfer, A. (1998) Three-dimensional segregation of supramolecular activation clusters in T cells. *Nature*. **395**, 82–86
16. Bromley, S. K., Burack, W. R., Johnson, K. G., Somersalo, K., Sims, T. N., Sumen, C., Davis, M. M., Shaw, A. S., Allen, P. M., and Dustin, M. L. (2001) The immunological synapse. *Annu. Rev. Immunol.* **19**, 375–396
17. Mócsai, A., Zhou, M., Meng, F., Tybulewicz, V. L., and Lowell, C. A. (2002) Syk is required for integrin signaling in neutrophils. *Immunity*. **16**, 547–558
18. Yan, S. R., Huang, M., and Berton, G. (1997) Signaling by adhesion in human neutrophils: activation of the p72syk tyrosine kinase and formation of protein complexes containing p72syk and Src family kinases in neutrophils spreading over fibrinogen. *J. Immunol.* **158**, 1902–1910
19. Auger, J. M. (2005) Adhesion of human and mouse platelets to collagen under shear: a unifying model. *FASEB J.* **19**, 825–827
20. Woodside, D. G., Oberfell, A., Leng, L., Wilsbacher, J. L., Miranti, C. K., Brugge, J. S., Shattil, S. J., and Ginsberg, M. H. (2001) Activation of Syk protein tyrosine kinase through interaction with integrin  $\beta$  cytoplasmic domains. *Curr. Biol.* **11**, 1799–1804
21. Woodside, D. G., Oberfell, A., Talapatra, A., Calderwood, D. A., Shattil, S. J., and Ginsberg, M. H. (2002) The N-terminal SH2 domains of Syk and ZAP-70 mediate phosphotyrosine-independent binding to integrin beta cytoplasmic domains. *J. Biol. Chem.* **277**, 39401–39408
22. Law, D. A., Nannizzi-Alaimo, L., Ministri, K., Hughes, P. E., Forsyth, J., Turner, M., Shattil, S. J., Ginsberg, M. H., Tybulewicz, V. L. J., and Phillips, D. R. (1999) Genetic and pharmacological analyses of Syk function in  $\alpha$ IIb $\beta$ 3 signaling in platelets. *Blood*. **93**, 2645–2652
23. Hughes, C. E., Finney, B. A., Koentgen, F., Lowe, K. L., and Watson, S. P. (2015) The N-terminal SH2 domain of Syk is required for (hem)ITAM, but not integrin, signaling in mouse platelets. *Blood*. **125**, 144–154

24. Clark, E. A., Shattil, S. J., Ginsberg, M. H., Bolen, J., and Brugge, J. S. (1994) Regulation of the protein tyrosine kinase pp72syk by platelet agonists and the integrin alpha IIb beta 3. *J. Biol. Chem.* **269**, 28859–28864
25. Shults, M. D., Janes, K. A., Lauffenburger, D. A., and Imperiali, B. (2005) A multiplexed homogeneous fluorescence-based assay for protein kinase activity in cell lysates. *Nat. Methods.* **2**, 277–284
26. Shults, M. D., Carrico-Moniz, D., and Imperiali, B. (2006) Optimal Sox-based fluorescent chemosensor design for serine/threonine protein kinases. *Anal. Biochem.* **352**, 198–207
27. Papp, E., Tse, J. K. Y., Ho, H., Wang, S., Shaw, D., Lee, S., Barnett, J., Swinney, D. C., and Bradshaw, J. M. (2007) Steady State Kinetics of Spleen Tyrosine Kinase Investigated by a Real Time Fluorescence Assay. *Biochemistry* . **46**, 15103–15114
28. Natsume, T., Koide, T., Yokota, S., Hirayoshi, K., and Nagata, K. (1994) Interactions between collagen-binding stress protein HSP47 and collagen. Analysis of kinetic parameters by surface plasmon resonance biosensor. *J. Biol. Chem.* **269**, 31224–31228
29. Yan, B. (2001) Calpain Cleavage Promotes Talin Binding to the beta 3 Integrin Cytoplasmic Domain. *J. Biol. Chem.* **276**, 28164–28170
30. Schmitz, R., Baumann, G., and Gram, H. (1996) Catalytic specificity of phosphotyrosine kinases Blk, Lyn, c-Src and Syk as assessed by phage display. *J. Mol. Biol.* **260**, 664–677
31. Fütterer, K., Wong, J., Grucza, R. A., Chan, A. C., and Waksman, G. (1998) Structural basis for syk tyrosine kinase ubiquity in signal transduction pathways revealed by the crystal structure of its regulatory SH2 domains bound to a dually phosphorylated ITAM peptide. *J. Mol. Biol.* **281**, 523–537
32. Ye, F., Petrich, B. G., Anekal, P., Lefort, C. T., Kasirer-Friede, A., Shattil, S. J., Ruppert, R., Moser, M., Fässler, R., and Ginsberg, M. H. (2013) The mechanism of Kindlin-mediated activation of Integrin  $\alpha$ IIb $\beta$ 3. *Curr. Biol.* **23**, 2288–2295
33. Morse, E. M., Brahme, N. N., and Calderwood, D. A. (2014) Integrin cytoplasmic tail interactions. *Biochemistry.* **53**, 810–820
34. Maartens, A. P., and Brown, N. H. (2015) The many faces of cell adhesion during Drosophila muscle development. *Dev. Biol.* **401**, 62–74
35. Castro, R. O. de, Zhang, J., Jamur, M. C., Oliver, C., and Siraganian, R. P. (2010) Tyrosines in the carboxyl terminus regulate Syk kinase activity and function. *J. Biol. Chem.* **285**, 26674–26684
36. Furlong, M. T., Mahrenholz, A. M., Kim, K.-H., Ashendel, C. L., Harrison, M. L., and Geahlen, R. L. (1997) Identification of the major sites of autophosphorylation of the murine protein-tyrosine kinase Syk. *Biochim. Biophys. Acta BBA - Mol. Cell Res.* **1355**, 177–190
37. Fitzgerald, D. J., Berger, P., Schaffitzel, C., Yamada, K., Richmond, T. J., and Berger, I. (2006) Protein complex expression by using multigene baculoviral vectors. *Nat. Methods.* **3**, 1021–1032
38. Gileadi, O., Burgess-Brown, N. A., Colebrook, S. M., Berridge, G., Savitsky, P., Smee, C. E. A., Loppnau, P., Johansson, C., Salah, E., and Pantic, N. H. (2008) High throughput production of recombinant human proteins for crystallography. *Methods Mol. Biol. Clifton NJ.* **426**, 221–246

FIGURES AND FIGURE LEGENDS

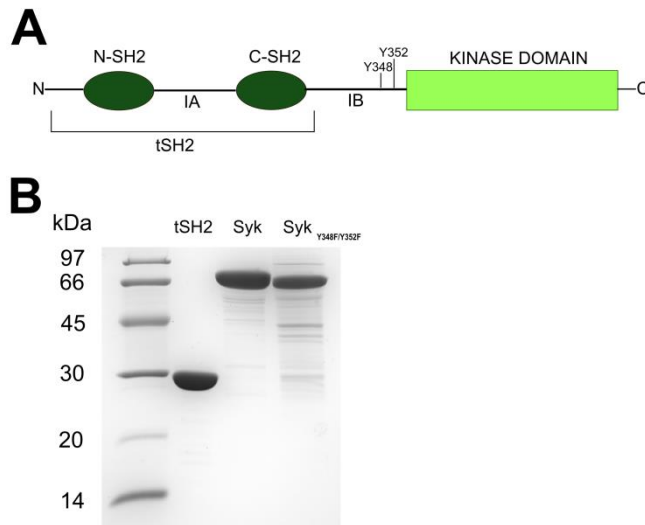


**FIGURE 1. (A)**, schematic representation of Syk kinase structure. The N-SH2 and C-SH2 are the regulatory domains which are connected to each other through Interdomain A (IA); they are named tandem SH2 (tSH2) together. tSH2 are connected to kinase domain via Interdomain B (IB). The tyrosines Y348 and Y352 get phosphorylated during protein activation and in this study they were mutated to phenylalanine. **(B)**, SDS-PAGE of purified proteins. For each protein preparation 5  $\mu$ g of protein was loaded on the gel.

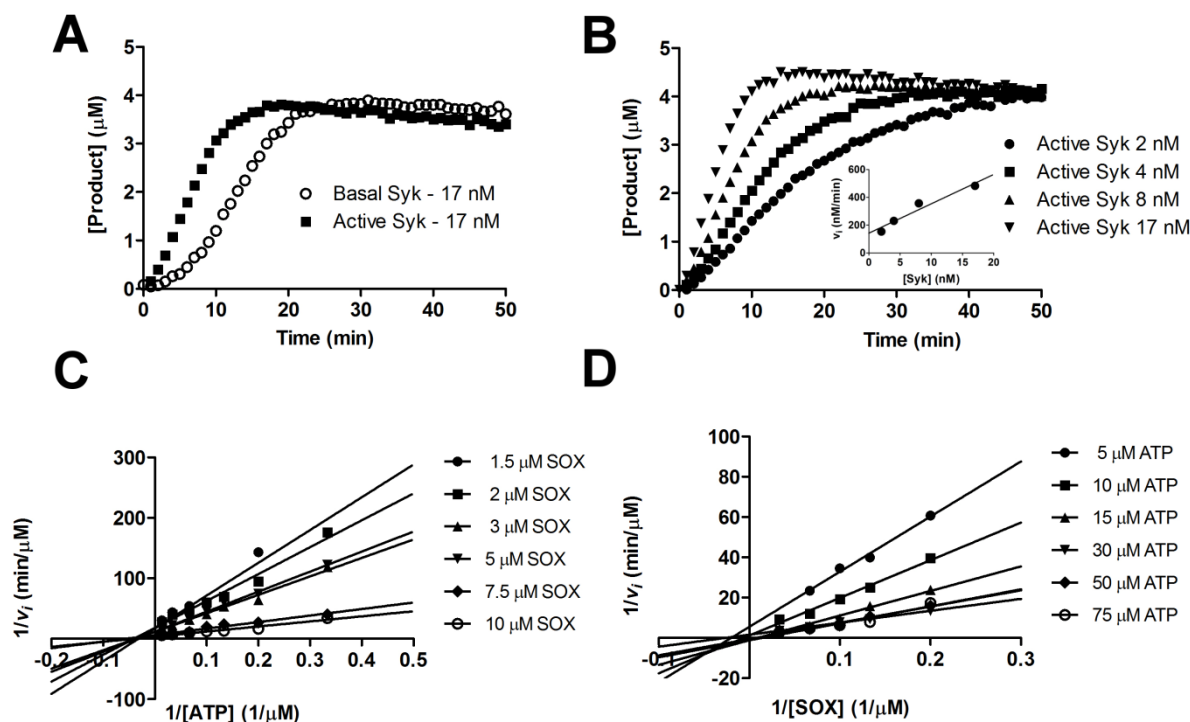


**FIGURE 2. Kinetic characterization of Syk kinase.** (A), Time course (min) of SOX peptide phosphorylation ( $\mu\text{M}$ ) for Basal Syk (*open circles*) and Active Syk (*squares*). Syk was activated through incubation with  $100 \mu\text{M}$  ATP at room temperature. The Syk activation was induced by incubation of the protein with ATP for 30 minutes. Basal Syk and Active Syk were used at the same concentration of  $17 \text{ nM}$ ; basal Syk showed a  $\sim 5$  minutes lag phase which was abolished in the active one. (B), Kinetic measurements of active Syk at different concentrations ( $2, 4, 8$  and  $17 \text{ nM}$ ). The inset shows the initial reaction speed ( $\text{nM}/\text{min}$ ) calculated using linear regression fit from 5 to 15 minutes plotted against Active Syk concentration ( $\text{nM}$ ). The calculated  $k_{\text{cat}}$  in this experiment was  $22 \pm 3 \text{ min}^{-1}$ . (C, D), Lineweaver-Burk plot generated from two-substrate analysis measurements of  $1/v_i$  vs  $1/[\text{ATP}]$  (C) and  $1/[\text{SOX}]$  (D). Experimental data were fit with ternary complex equation and calculated  $K_m$  was  $6 \pm 1 \mu\text{M}$  for SOX peptide and  $29 \pm 3 \mu\text{M}$  for ATP.

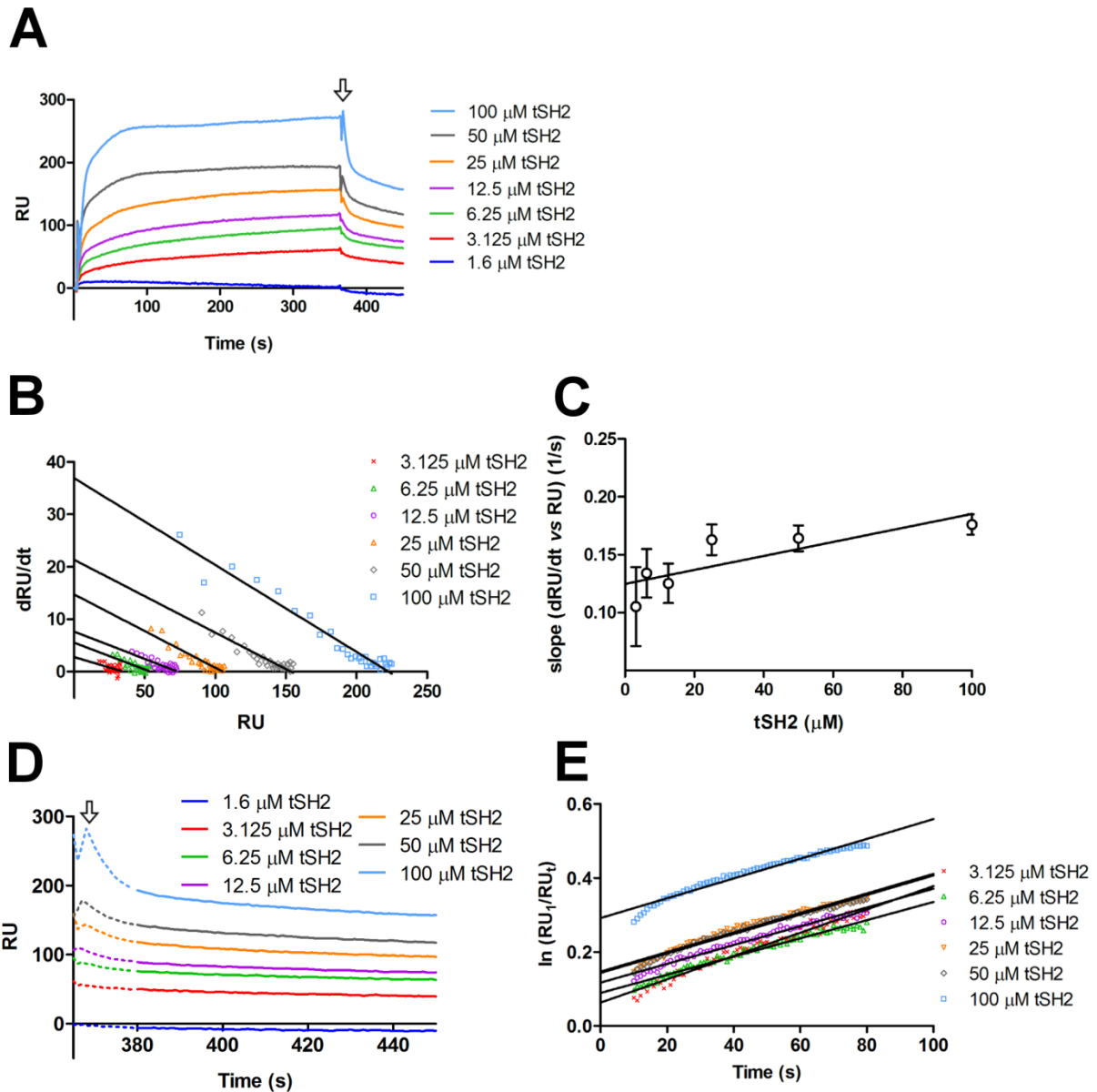


**FIGURE 3. Interaction between tSH2 and Integrin  $\beta_3$  tail.** (A), Surface Plasmon Resonance (SPR) experiment where integrin  $\beta_3$  tail peptide was coupled on the surface (ligand) and different concentrations of tSH2 (from 1.3 to 100  $\mu\text{M}$ ) were injected (analyte). In the graph is plotted the variation of Response Unit (RU) in the time (seconds) for each tSH2 concentration tested. The arrow indicates the stop of the injection and, therefore, the beginning of the dissociation phase. (B), dRU/dt (variation of RU in time) plotted against RU (from 10 to 30 seconds of the association curve, see panel A). Solid lines correspond to best linear regressions calculated for each tSH2 concentration. (C), Calculation of association rate constant ( $k_{on}$ ) of the tSH2-integrin  $\beta_3$  tail peptide complex formation. Error bars are derived from linear regression analysis of B panel in this figure (see *Experimental procedure*). (D), Variation of RU in the time (seconds) of the dissociation phase. The arrow indicates the end of injection as in panel A. The dotted line corresponds to the part of dissociation curve which was not used for the determination of the dissociation rate constant (see panel E), while the solid line indicates the part which was used. (E), Variation of  $\ln(RU_1/RU_t)$  in the time (seconds), the best linear fits are represented with solid lines.  $RU_1$  indicates the response units at the beginning of dissociation phase, and  $RU_t$  indicates



the response units at the time  $t$ . The slope of the linear regression corresponds to dissociation rate constant ( $k_{\text{off}}$ ) (see *Experimental procedure*).

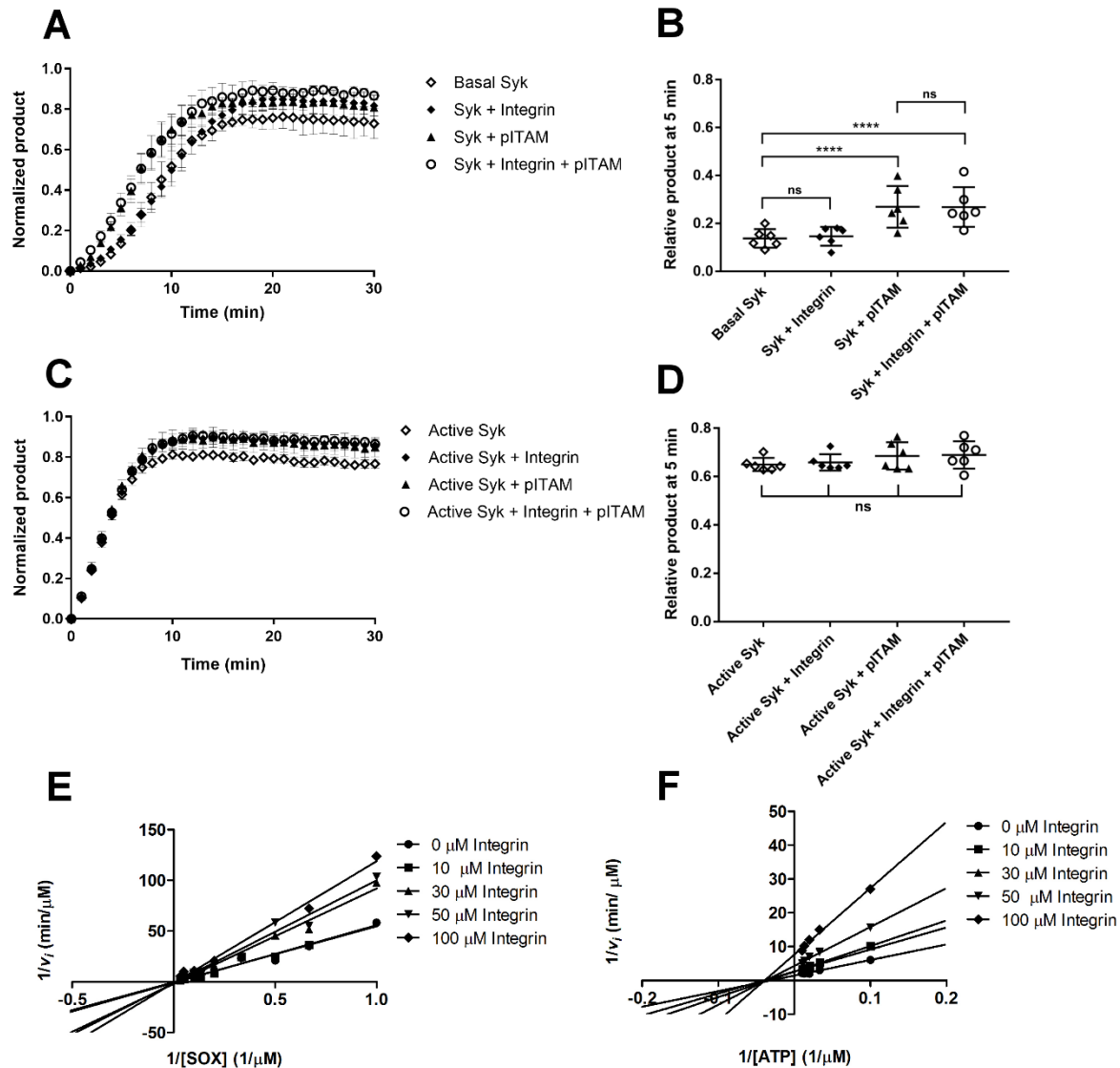


**FIGURE 4. Effect of pITAM and Integrin  $\beta_3$  tail on Syk wild type activity.** (A) Kinetic measurement of Basal Syk in absence of peptide (*open diamonds*), in presence of 30  $\mu\text{M}$  integrin  $\beta_3$  cytoplasmic tail peptide (*diamonds*), 10  $\mu\text{M}$  pITAM peptide (*triangles*) and combination of both (*open circles*). The activity is expressed in terms of normalized product formation in the time (min); basal Syk was used at concentration of 17 nM. Error bars correspond to the standard deviation calculated from six different experiments. (B) ANOVA analysis of the 5 min time point in experiment shown in panel A. The data indicate that the presence of soluble pITAM activates the protein reducing the lag-phase of basal Syk. P value for basal Syk vs Syk + pITAM and basal Syk vs Syk + pITAM + Integrin were both  $<0.0001$ . Comparing the basal Syk vs Syk + Integrin and the Syk + pITAM vs Syk + Integrin + pITAM with ANOVA test resulted in non-significant (ns) P values thus showing that soluble integrin  $\beta_3$  cytoplasmic tail peptide had no effect. (C) Kinetic measurement of active Syk in absence of peptide (*open diamonds*), in presence of 30  $\mu\text{M}$  integrin  $\beta_3$  cytoplasmic tail peptide (*diamonds*), 10  $\mu\text{M}$  pITAM peptide (*triangles*) and combination of both (*open circles*). The activity is expressed in terms of normalized product formation in the time (min). Active Syk was used at concentration of 17 nM. (D) The ANOVA analysis of the 5 min time point in panel C; it resulted in a non-significant (ns) P value suggesting that the pre-activated Syk is not modulated by the presence of either of two peptides. (E, F) Lineweaver–Burk plots showing the competitive inhibition towards SOX peptide (E) and uncompetitive inhibition towards ATP (F).

(F) by integrin  $\beta_3$  cytoplasmic tail. In each case  $1/v_i$  was plotted against  $1/[\text{SOX}]$  (E) or  $1/[\text{ATP}]$  (F). The experiments were carried out using active Syk at concentration of 4 nM.

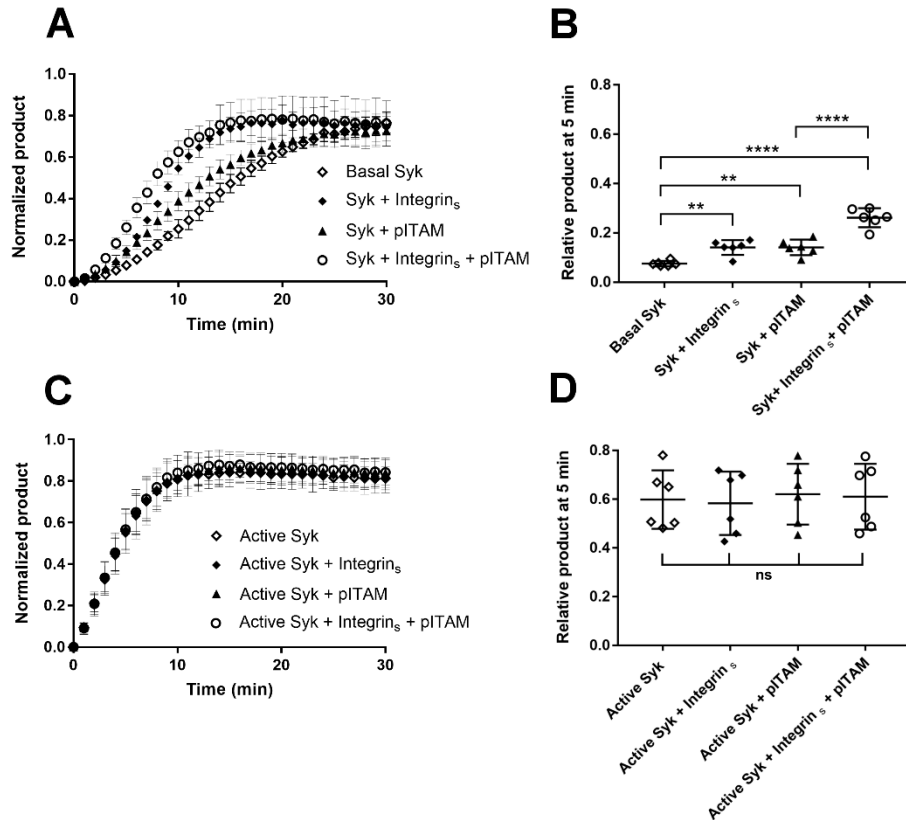


**FIGURE 5. Effect of clustered integrin  $\beta_3$  cytoplasmic tails on Syk activation. (A)** Time course (min) of the normalized product formation in absence of peptides (*open diamonds*) and in presence of integrin  $\beta_3$  cytoplasmic tail peptide coupled on the assay plate surface (*diamonds*), 10  $\mu$ M pITAM (*triangles*) and combination of the two peptides (*open circles*). Basal Syk was used at 17 nM. Error bars correspond to the standard deviation calculated using six different experiments. **(B)** ANOVA analysis of the 5 min time point in panel A. The experiment shows that surface-bound integrin peptide reduces the lag phase of basal Syk; P value for basal Syk vs Syk + Integrin<sub>s</sub> was 0.0014 and it is comparable with the P value for basal Syk vs Syk + pITAM which was 0.0013. Combination of two peptides further accelerated the process (P value <0.0001). Integrin  $\beta_3$  cytoplasmic tail bound on plate surface has also a synergic effect in presence of pITAM peptide in fact comparing the Syk + pITAM vs Syk + pITAM + Integrin<sub>s</sub> the ANOVA test gave a P value <0.0001. **(C)** Time course (min) of the normalized product formation in absence of peptides (*open diamonds*) and in presence of integrin  $\beta_3$  cytoplasmic tail peptide coupled on the assay plate surface (*diamonds*), 10  $\mu$ M pITAM (*triangles*) and combination of two peptides (*open circles*). Active Syk was used at 17 nM. **(D)** ANOVA analysis of the experiment showed in panel C. P values were calculated using ANOVA test including six separate experiments using the relative product formed at 5 min time point as described in *Experimental procedure*. P values were non-significant (ns).

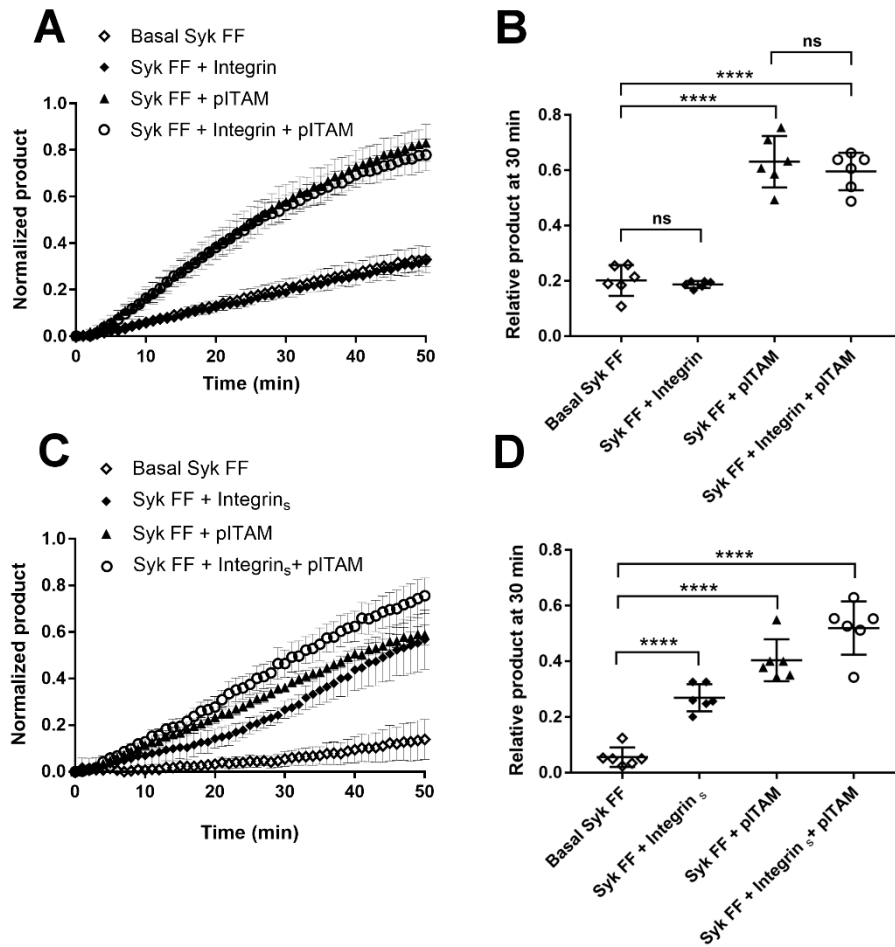


**FIGURE 6. Effect of pITAM and clustered integrin  $\beta_3$  tails on Syk Y348F/Y352F mutant activation.** **(A)** Kinetic measurement of Syk mutant activity in absence of peptides (*open diamonds*), 30  $\mu$ M integrin  $\beta_3$  tail peptide (*diamonds*), 10  $\mu$ M pITAM (*triangles*), and combination of both peptides (*open circles*). Syk FF was used at 17 nM concentration and the error bars are derived from the calculated standard deviation from six different experiments. **(B)** ANOVA analysis of the 30 min time point in panel A. Comparison of basal Syk FF vs Syk FF + Integrin and the Syk FF + pITAM vs Syk FF + Integrin + pITAM revealed that the soluble Integrin peptide does not activate Syk FF (P value non-significant - ns) in contrast to pITAM (P values <0.0001). **(C)** Same experiment described in panel A, except for Integrin  $\beta_3$  tail peptide which was coupled on the plate surface. **(D)** ANOVA analysis of the 30 min time point in panel C. All P values were <0.0001.

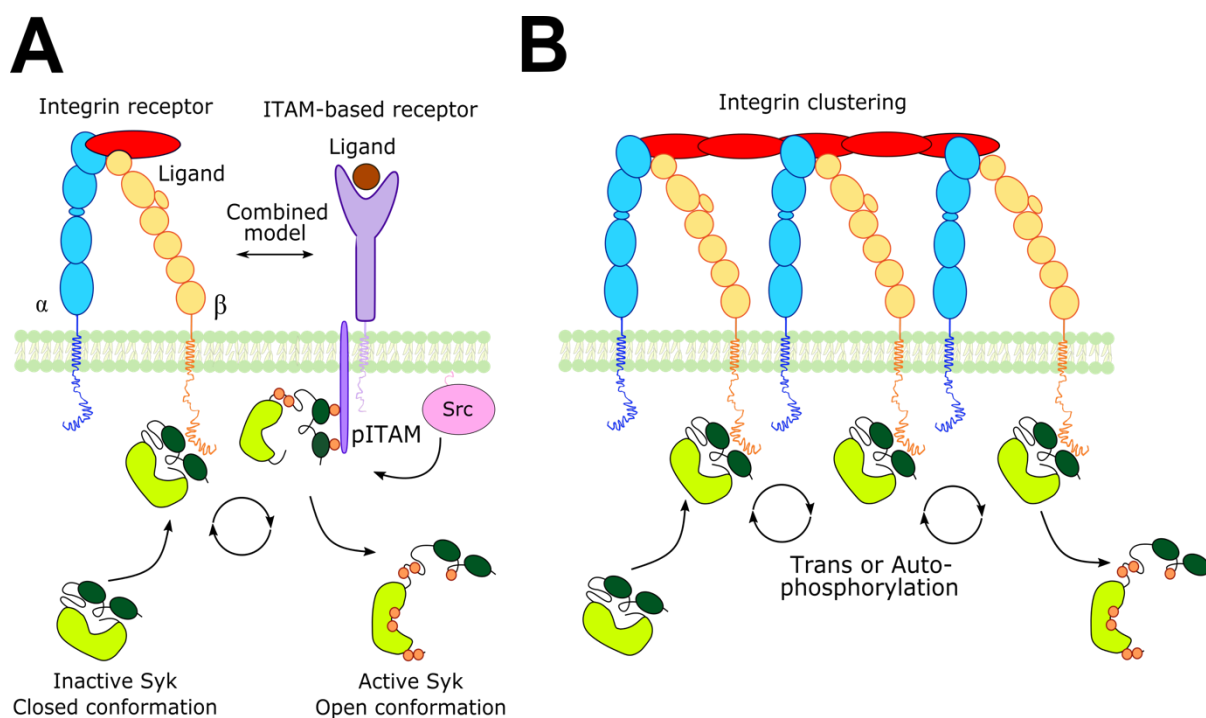


**FIGURE 7. A model of Syk activation mediated by clustered Integrins.** Integrin receptor subunits  $\alpha$  and  $\beta$  are represented in blue and yellow, respectively. ITAM containing receptor is in purple. Src family kinase is represented in pink; Lyn kinase is the Src kinase which is mainly involved in Syk activation procedure. Syk is represented in two conformations (closed and open). The kinase domain is light green while the SH2 domains are in dark green, black lines indicate the linker regions. The small orange circles represent the phosphorylations along the Syk structure. **A.** Combined model of Syk activation mediated by integrin and ITAM-containing receptors. Syk is recruited near the membrane by the interaction with integrin tail and phosphorylated ITAM. Syk is first activated by interaction with pITAM through conformational rearrangement in the kinase structure. Then it can be phosphorylated by other kinases recruited via integrin pathway. Src-family kinases may be responsible for the phosphorylation of both ITAM receptor and Syk. **B.** Syk activation model mediated by integrin clustering. Inactive Syk can interact with integrin tail. The proximity effect enhances Syk trans/autophosphorylation activity leading to Syk activation. Importantly, this pathway can occur independently of pITAM and Src family kinases.

**Phosphorylated immunoreceptor tyrosine-based activation motifs and integrin cytoplasmic domains activate spleen tyrosine kinase via distinct mechanisms**

Lina Antenucci, Vesa P. Hytönen and Jari Ylännö

*J. Biol. Chem.* published online February 12, 2018

---

Access the most updated version of this article at doi: [10.1074/jbc.RA117.000660](https://doi.org/10.1074/jbc.RA117.000660)

Alerts:

- [When this article is cited](#)
- [When a correction for this article is posted](#)

[Click here](#) to choose from all of JBC's e-mail alerts